

# Operation of Thermoacoustic Stirling Heat Engine Driven Large Multiple Pulse Tube Refrigerators

**Bayram Arman, John Wollan, and Vince Kotsubo**

Praxair, Inc.  
Tonawanda, NY 14150

**Scott Backhaus and Greg Swift**

Los Alamos National Laboratory  
Los Alamos, NM 87545

## ABSTRACT

With support from Los Alamos National Laboratory, Praxair has been developing thermoacoustic Stirling heat engines and refrigerators for liquefaction of natural gas. The combination of thermoacoustic engines with pulse tube refrigerators is the only technology capable of producing significant cryogenic refrigeration with no moving parts. A prototype, powered by a natural-gas burner and with a projected natural-gas-liquefaction capacity of 500 gal/day, has been built and tested. The unit has liquefied 350 gal/day, with a projected production efficiency of 70% liquefaction and 30% combustion of an incoming gas stream. A larger system, intended to have a liquefaction capacity of 20,000 gal/day and an efficiency of 80 to 85% liquefaction, has undergone preliminary design.

In the 500 gal/day system, the combustion-powered thermoacoustic Stirling heat engine drives three pulse tube refrigerators to generate refrigeration at methane liquefaction temperatures. Each refrigerator was designed to produce over 2 kW of refrigeration. The orifice valves of the three refrigerators were adjusted to eliminate Rayleigh streaming in the pulse tubes. This paper describes the hardware, operating experience, and some recent test results.

## INTRODUCTION

Praxair has been developing thermoacoustic liquefiers and refrigerators for liquefaction of natural gas and for other cryogenic applications. The liquefier development program is divided into two components: pulse tube refrigerators driven by combustion-powered thermoacoustic Stirling heat engines (TASHEs), and pulse tube refrigerators driven by linear motors. For the foreseeable future, the linear-motor-driven technology will be limited to low-power refrigeration and liquefaction applications.

Praxair's efforts to develop practical high-power combustion-driven thermoacoustic natural-gas liquefaction to eliminate the need for significant electric power in multi-kW cryogenic refrigeration

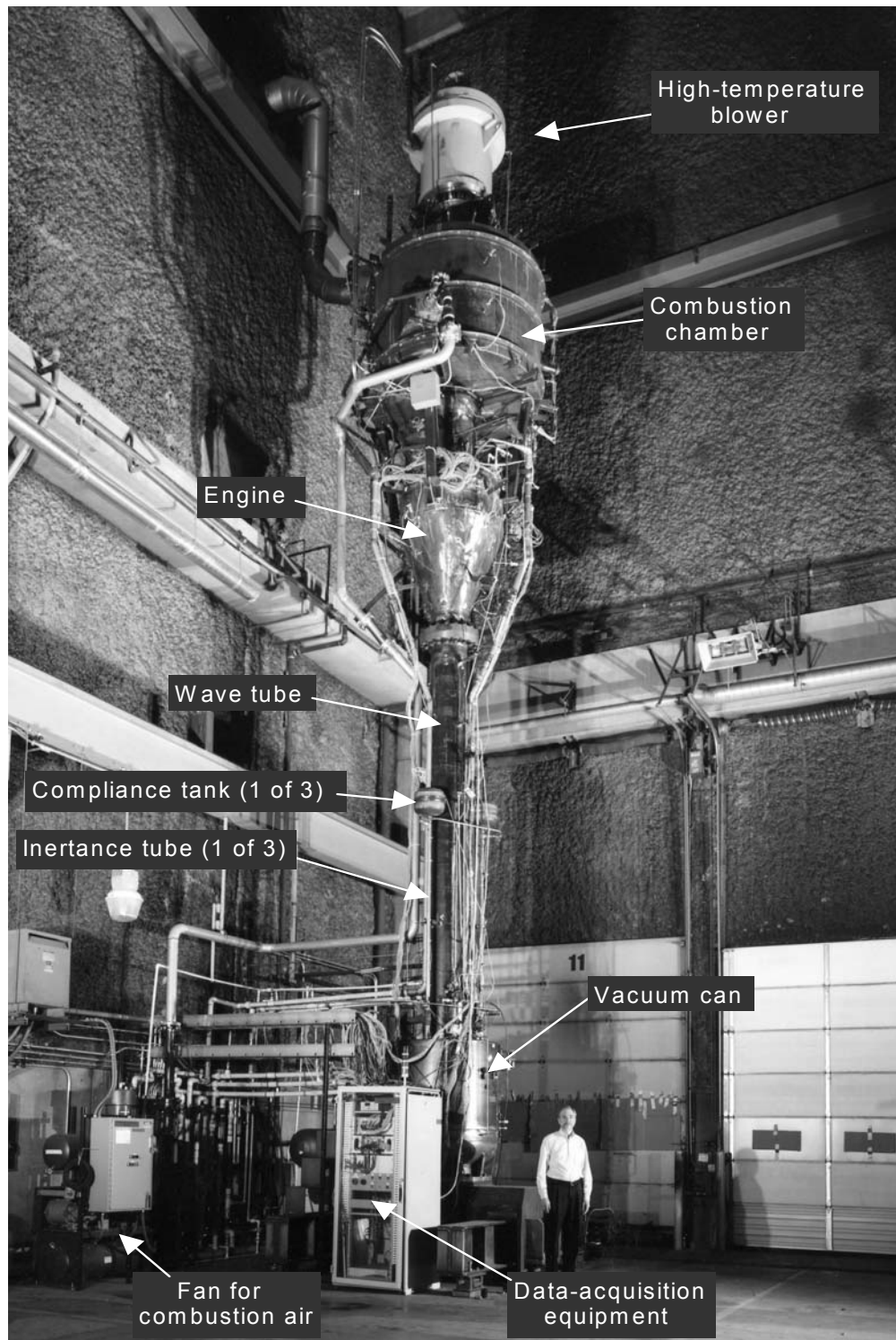


**Figure 1.** Photograph of 500-gal/day system in Denver, with project leader John Wollan.

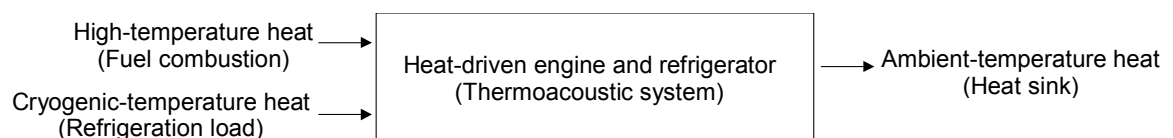


**Figure 2.** Simplest block diagram of the engine-driven refrigerator system. Heat is pumped from cryogenic temperature, high-temperature heat is consumed, and waste heat is rejected to ambient temperature, without any moving parts.

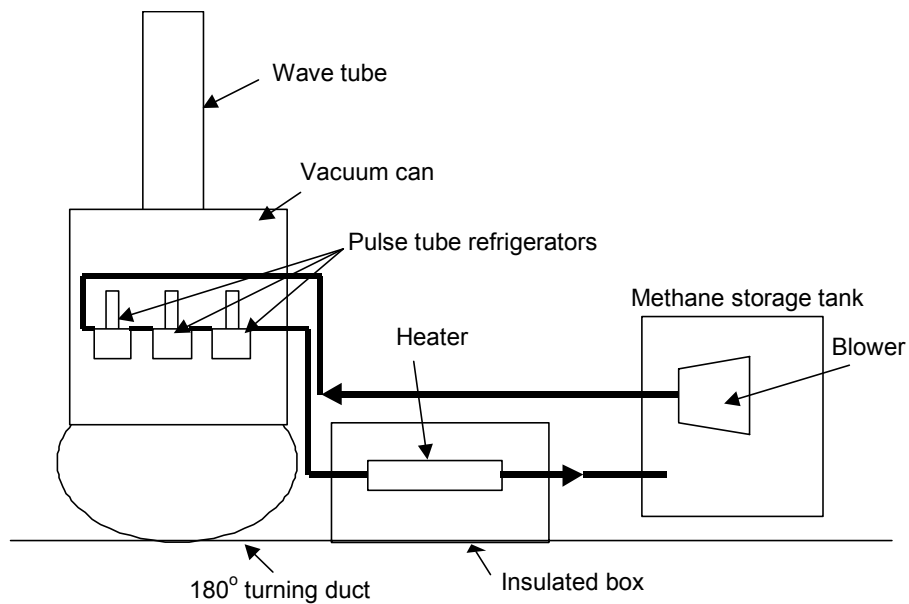


**Figure 3.** Pulse tube refrigerators and methane circulation loop.

eration began with its 2001 acquisition of the project from Chart, Inc. Chart's development effort was summarized by Wollan et al.<sup>1</sup> and Swift and Wollan.<sup>2</sup> After Praxair's acquisition of the project, extensive modifications were made to the acquired hardware: The refrigerators were kept intact, but the engine and burner were completely rebuilt, and a more sophisticated system for control and data acquisition was created.

The resulting system is shown in Figure 1, and a simple block diagram is shown in Figure 2. Heat from a high-temperature heat source (combustion of natural gas) provides useful energy to the system, heat is removed from a load (methane, experiencing cooling and liquefaction) at cryogenic temperatures, and waste heat is rejected to ambient temperature. Thermoacoustic processes in 30-bar helium gas accomplish the energy conversions and transport.

The major thermoacoustic subsystems are: (1) an engine to generate high-intensity acoustic power from high-temperature heat; (2) a wave tube (a nearly half-wavelength resonator) to transport the acoustic power from the engine to the refrigerators and to determine the 40-Hz operating frequency; and (3) refrigerators to generate useful cryogenic refrigeration while consuming the acoustic power. The engine is a thermoacoustic–Stirling hybrid heat engine.<sup>3</sup> The engine subsystem includes additional components to generate heat and transport it to the hot heat exchanger of the engine: a combustion chamber and a high-pressure, high-temperature, blower-driven<sup>4</sup> circulating-helium heat-transfer loop. The refrigerators are three inertance-enhanced orifice pulse tube refrigerators. A methane circulation loop provides the refrigeration load for the refrigerators. A cooling-water loop provides the ambient-temperature sink for the engine and the refrigerators.

This paper focuses on the pulse tube refrigerators and their performance. As shown schematically in Figure 3, the three refrigerators are driven in parallel by the acoustic power delivered by the wave tube. They are linked in series by the methane circulation loop, so that the first refrigerator precools the incoming methane to about 180 K, the second refrigerator cools the methane to liquefaction temperature and partially liquefies it, and the third refrigerator further liquefies the methane.

For thermal isolation, the three refrigerators are wrapped in a few cm of fine fiber insulation and enclosed in a single vacuum jacket pumped to about 10 microns. The three refrigerators are mounted on an annular 180° turning duct at the bottom of the wave tube. The refrigerators have similarities to the one that was used in the Cryenco–Los Alamos TADOPT project,<sup>5</sup> with stainless-steel screen regenerators and tube-in-shell heat exchangers. A valve in series with each refrigerator's inertance enables phase adjustments. Initially, the inertance tubes were not water

cooled and they ran so hot that the reduced gas density in them provided insufficient inertance for efficient refrigerator operation. For the measurements reported here, the tubes were water-jacketed.

These three pulse tube refrigerators were designed to produce a total of 7 kW of refrigeration at methane liquefaction temperatures, so they are large, with regenerators of 20 cm diameter and pulse tubes of 10 cm diameter. All components are in line in each refrigerator, in the following sequence starting from the bottom: aftercooler, regenerator, cold heat exchanger, pulse tube, secondary ambient heat exchanger, orifice valve, inertance tube, compliance tank.

The third refrigerator is 3.4 cm lower than the second, to allow flow of condensed liquid methane from the second refrigerator's cold heat exchanger into the third refrigerator's cold heat exchanger via gravity without deep accumulation of liquid in the second refrigerator. The third refrigerator's cold heat exchanger has a liquid-level sensor.

The instrumentation on the refrigerators was kept to a minimum. Three pressure transducers<sup>6</sup> are located near the pressure node at the middle of the wave tube for measuring acoustic power<sup>7</sup> delivered to the lower half of the wave tube and the refrigerators. A fourth pressure transducer is mounted in the 180° turning duct, the common space at the entrance to the three refrigerator aftercoolers. Each refrigerator also has a pressure transducer in its compliance tank and at the top of its pulse tube, between the secondary ambient heat exchanger and the orifice valve.

Each pulse tube has three equally spaced thermocouples along its wall to indicate<sup>8,9</sup> pulse-tube streaming, which is discussed below. Several more thermocouples are mounted on the axial midpoints of the regenerators, on the inertance of the third refrigerator, and throughout the methane circulation loop.

Three separate cooling water streams are provided for the aftercoolers, the secondary ambient heat exchangers, and the water jackets around the inertance tubes. Flow meters are located in each of these three streams, to measure the total flow to the three aftercoolers, the three ambient heat exchangers, and the three water jackets, but the individual water flow rates are not measured.

A pressure-regulated, closed-loop methane circulating system provides the load on the refrigerators. This methane system, shown schematically in Figure 3, consists of a large storage tank, a circulating blower, a heater enclosed in an insulated box, and the associated drive and control electronics. The heater consists of three electric-resistance cartridges enclosed in tubes carrying the methane. The cooling power of the refrigerators is determined by measuring the electrical power required by this heater to vaporize the liquefied methane and reheat it back to the initial inlet-methane temperature. (The cooling power does not uniquely determine the liquefaction rate unless there is 100% liquefaction.) The methane pressure sets the cold-end temperature of the third refrigerator whenever there is a liquid-vapor interface in its cold heat exchanger.

## EXPERIMENTS AND OVERALL PERFORMANCE

In a typical run, the burner is ignited to heat the hot heat exchanger of the engine to start the acoustic oscillations. During the engine startup, the refrigerator orifice valves are closed so there is negligible refrigeration, and the acoustic power produced by the engine is dissipated mostly in wave-tube losses. Once the desired acoustic amplitude is reached, the refrigerators' orifice valves are gradually opened to start refrigeration. Opening the orifice valves also increases the load on the engine, which causes a rise in the hot temperature of the engine and demands an increased fuel flow rate to the combustion system to maintain the desired acoustic amplitude. The engine operation is very stable and controllable. It typically takes two hours to go from one operating point to another and settle down to a sufficiently time-independent state that "steady-state" data can be acquired.

During attempts to reach performance goals, the highest system cooling power to date was 3800 W at 150 K, the temperature being determined by the methane pressure of 150 psia. This cooling power corresponds to 350 gal/day of liquefaction (though in fact the methane flow rate was greater than this, so the methane stream leaving the third refrigerator was less than 100%

liquid). Greater liquefaction rates and cooling powers have been prevented by a power handicap in the thermoacoustic engine, due to unforeseen inertance associated with end effects at some locations in the engine. These inertial effects can be avoided, or taken into account, in future hardware designs.

The power shortfall does not seriously affect the thermoacoustic efficiency. At the 350-gal/day operating point, a direct comparison of the refrigeration power to the rate at which fuel was fed to the burner yields an overall system efficiency of 45% liquefied, 55% burned. In other words, 45% of a pure methane stream arriving at the system would have been delivered as liquefied product, and 55% would have been burned, if pure methane instead of natural gas had been used as fuel for the burner. However, most of the combustion heat was lost up the flue and to heat leak from the combustion chamber, because no effort was made to minimize such losses in this hardware. A standard flue-gas recuperator and better combustion-chamber insulation, both needed for a commercially interesting system, would enable the delivery of 85% of the heat of combustion to the thermoacoustic engine. In this reasonably plausible imaginary situation, the efficiency at the 350 gal/day operating point would have been 70% liquefied, 30% burned.

## SOME DETAILED PULSE TUBE REFRIGERATOR RESULTS

Experiments measuring the refrigeration power spanned many combinations of refrigerator orifice-valve openings, acoustic pressure amplitudes, and methane pressures. Although DeltaE<sup>10</sup> was used to design these refrigerators, the Sage program<sup>11</sup> was used to analyze and interpret the test results. (Whenever we have compared the results of these two codes, they have been similar.) Measured pressure amplitudes and phases, including the pressure differences across the regenerators, agreed reasonably well with the Sage models. Measured cooling powers were significantly below the Sage predictions.

In this paper, we present some details regarding streaming in the third refrigerator's pulse tube, while the orifice valves of the other two refrigerators were closed. A Sage inertance-network model was used to infer the volume flow rates from the measured pressures. In the Sage model, the oscillating mass flow at the entrance to the network and the valve opening were adjusted until the calculated pressure amplitudes matched the measured values in the compliance tank and at the top of the pulse tube. To establish confidence in this model, Figure 4 displays the good agreement between the measured and calculated differences between the pressure phases in the compliance tank and at the top of the pulse tube, as a function of the orifice-valve setting, for three different acoustic pressure amplitudes. In our notation,  $p_m$  is the mean pressure and  $|p_1|$  is the amplitude of the fundamental component of the oscillating pressure.

With confidence established in the Sage model, it can be used to predict the phase difference between the pressure  $p_1$  and volume flow rate  $U_1$ , which is a key parameter in the analysis of heat transport via Rayleigh streaming in pulse tubes by Olson and Swift.<sup>12</sup> According to their analysis, the streaming flow is minimized if the  $U_1$ - $p_1$  phase difference somewhere near the middle of the pulse tube is  $-50^\circ$ , which corresponds in these refrigerators to a phase difference at the ambient end of the pulse tube ranging from  $-55^\circ$  to  $-60^\circ$ .

One obvious indication of minimum streaming is a linear pulse-tube temperature profile.<sup>8,9</sup> Using the three equally spaced thermocouples on the side of the pulse tube, a linear profile occurs when the normalized temperature,  $1 - 2T_{\text{mid}}/T_{\text{average}}$ , equals zero. In Figure 5, the normalized temperature is plotted versus the  $U_1$ - $p_1$  phase difference at the ambient end of the pulse tube. The temperature profiles become linear within about  $10^\circ$  of the expected phase difference, confirming that Olson and Swift's analysis is at least approximately applicable to these refrigerators.

Further confirmation of streaming suppression can be seen in the coefficient of performance (COP). The COP is the ratio of measured cooling power to modeled aftercooler input acoustic power, with the latter confirmed by measurements of the acoustic power<sup>7</sup> at the middle of the wave tube. The COP should be a maximum when streaming is minimized. Figure 6 displays the COP versus the  $U_1$ - $p_1$  phase difference, showing the maximum COP occurring at about the same phase difference as that yielding a linear pulse-tube temperature profile in Figure 5.

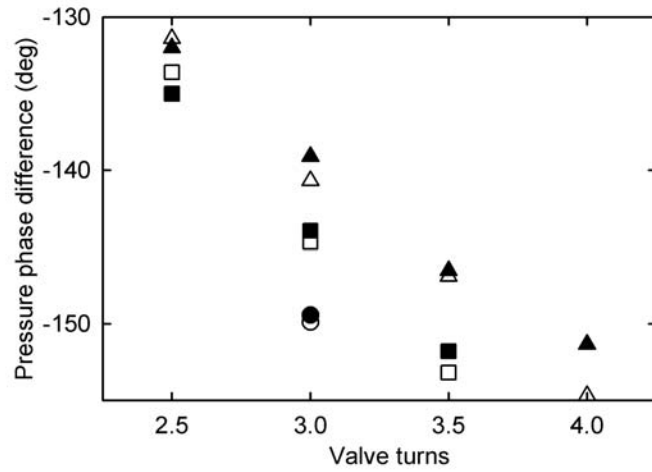


**Figure 4.** Compliance pressure phase minus pulse-tube pressure phase in the third refrigerator. Circles,  $|p_1|/p_m = 3\%$ , squares 5%, triangles 7%. Filled symbols represent experimental data, and open symbols represent Sage calculations.

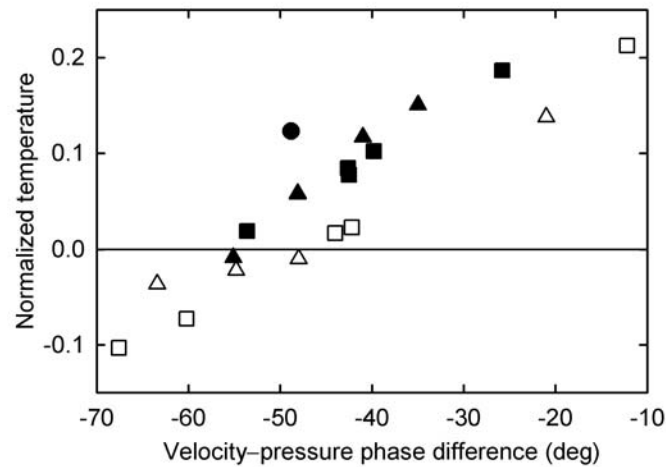


**Figure 5.** Normalized temperature vs.  $U_1-p_1$  phase difference in the third refrigerator. Circle,  $|p_1|/p_m = 3\%$ , squares,  $|p_1|/p_m = 5\%$ , triangles 7%. The filled and open symbols represent data taken in different months. Filled symbols correspond to those of Figure 4.

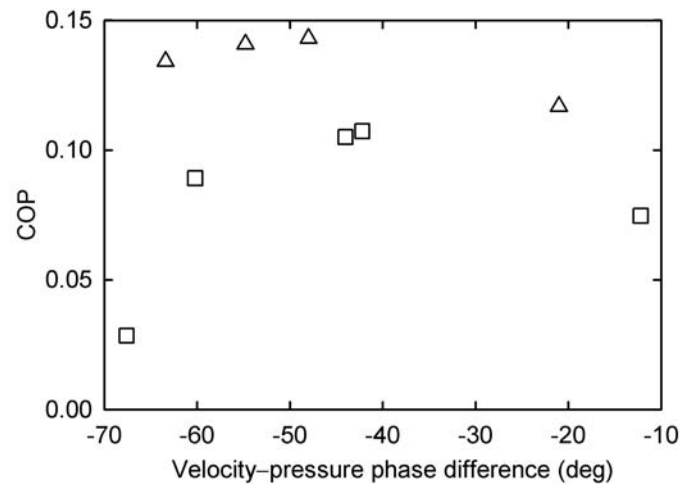


**Figure 6.** Coefficient of performance vs.  $U_1-p_1$  phase difference for the data represented by open symbols in Figure 5.

## CONCLUSIONS AND RECOMMENDATIONS

The multiple Stirling heat engine-driven pulse tube refrigerators run well and stably. Pressure amplitudes and phases, and regenerator pressure drops, agree reasonably well with computer models. A more extensive and comprehensive experimental study is needed for further improvement in the agreement between the predictions and experiments.

The inertance networks behave as expected. Water-cooling the inertance tube and orifice valve in pulse tube refrigerators of this size is essential to keep the gas density high enough to provide the expected inertance. Orifice valve adjustment easily allows minimization of pulse-tube streaming, as demonstrated by linear pulse-tube temperature profiles and maximization of the COP, at operating points close to those expected.

These analyses indicate that inertance models in programs like Sage<sup>11</sup> and DeltaE<sup>10</sup> are adequate for the turbulent flows in the inertances of large pulse tube refrigerators.

As with all large pulse tube refrigerators that have been manufactured and tested by our team, these three refrigerators do not perform as well as expected. At  $|p_1|/p_m = 7\%$ , the COPs are 30% below Sage's predictions.

Future experiments towards understanding regenerator internal streaming and other complex behavior are needed to improve understanding of such large pulse tube refrigerators. A vibration-balanced pair of CFIC's Q-Drive pressure wave generators<sup>13</sup> would be suitable for driving one of these three refrigerators.

The Los Alamos–Praxair team has made steady improvements in the thermoacoustic natural gas liquefaction system's efficiency:

- Coolahoop (NIST–Los Alamos)<sup>14</sup>  
10% liquefy, 90% burn (predicted from measured electrical heats)
- 140-gal/day TADOPTR (Los Alamos–Cryenco)<sup>5</sup>  
40% liquefy, 60% burn
- 500-gal/day TASHE-OPTR (the hardware described in this paper)  
70% liquefy, 30% burn (assuming a flue recuperator is used)
- 20,000-gal/day Cascade-OPTR<sup>15</sup> (current Los Alamos–Praxair preliminary design)  
80–85% liquefy, 15–20% burn

The planned 20,000 gal/day thermoacoustic liquefier technology should be able to compete with existing natural-gas liquefiers of comparable capacity, in terms of both efficiency and cost.

## REFERENCES

1. Wollan, J.J., Swift, G.W., Backhaus, S.N., and Gardner, D.L., "Development of a Thermoacoustic Natural Gas Liquefier," *Proceedings of AIChE Meeting*, New Orleans LA, March 11-14 (2002). Also available at [www.lanl.gov/thermoacoustics/Pubs/Wollan.pdf](http://www.lanl.gov/thermoacoustics/Pubs/Wollan.pdf)
2. Swift, G.W., and Wollan, J.J. "Thermoacoustics for liquefaction of natural gas," *GasTIPS*, vol. 8(4), (Fall 2002), pp. 21-26. Also available at [www.lanl.gov/thermoacoustics/Pubs/GasTIPS.pdf](http://www.lanl.gov/thermoacoustics/Pubs/GasTIPS.pdf)
3. Backhaus, S.N., and Swift, G.W., "A Thermoacoustic-Stirling Heat Engine." *Nature*, vol. 399, (1999), pp. 335-338; "A thermoacoustic-Stirling heat engine: Detailed study," *Journal of the Acoustical Society of America*, vol. 107 (2000), pp. 3148-3166.
4. Piller Industrieventilatoren GmbH, Moringen, Germany, [www.piller.de](http://www.piller.de)
5. Swift, G.W., Allen, M.S., and Wollan, J.J., "Performance of a tapered pulse tube," *Cryocoolers 10*, Kluwer Academic/Plenum Publishers, New York (1999), pp. 315-320.
6. Endevco, Inc., San Juan Capistrano CA, model 8510B-500.
7. Fusco, A.M., Ward, W.C., and Swift, G.W., "Two-sensor power measurements in lossy ducts," *Journal of the Acoustical Society of America*, vol. 91 (1992), pp. 2229-2235.

8. Duband, L., Charles, I., Ravex, A., Miquet, L., and Jewell, C., "Experimental results on inertance and permanent flow in pulse tube coolers," *Cryocoolers 10*, Kluwer Academic/Plenum Publishers, New York (1999), pp. 281-290.
9. Kotsubo, V., Huang, P., and Nast, T.C., "Observation of DC flows in a double inlet pulse tube," *Cryocoolers 10*, Kluwer Academic/Plenum Publishers, New York (1999), pp. 299-305.
10. Ward, W.C., and Swift, G.W., "Design Environment for Low Amplitude Thermoacoustic Engines (DeltaE)," *Journal of the Acoustical Society of America*, vol. 95 (1994), pp. 3671-3672. Software and user's guide available either from the Los Alamos thermoacoustics web site [www.lanl.gov/thermoacoustics/](http://www.lanl.gov/thermoacoustics/) or from the Energy Science and Technology Software Center, US Department of Energy, Oak Ridge, Tennessee.
11. Gedeon, D., "A globally implicit Stirling cycle simulation," *Proceedings of the 21st Intersociety Energy Conversion Engineering Conference*, American Chemical Society (1986), pp. 550-554. Sage Version 3.0 software and user's guide available from Gedeon Associates, Athens, Ohio.
12. Olson, J.R., and Swift, G.W., "Acoustic streaming in pulse tube refrigerators: Tapered pulse tubes," *Cryogenics*, vol. 37, (1997), pp. 769-776; "Suppression of acoustic streaming in tapered pulse tubes," *Cryocoolers 10*, Kluwer Academic/Plenum Publishers, New York (1999), pp. 307-313.
13. CFIC, Inc., 302 Tenth St., Troy NY 12180, [www.qdrive.com](http://www.qdrive.com).
14. Radebaugh, R., McDermott, K.M., Swift, G.W., and Martin, R.A., "Development of a thermoacoustically driven orifice pulse tube refrigerator," *Proceedings of the Interagency Meeting on Cryocoolers*, October 24, 1990, Plymouth, Massachusetts, David Taylor Research Center publication 91/003, Bethesda MD 20084-5000, pp. 205-220.
15. Gardner, D.L., and Swift, G.W., "A cascade thermoacoustic engine," *Journal of the Acoustical Society of America*, vol. 114 (2003), pp. 1905-1919.